SPACE TELESCOPE SCIENCE INSTITUTE
Operated for NASA by AURA

Instrument Science Report WFC3 2005-22

Results of WFC3 Thermal Vacuum Testing - IR Channel Ghosts & Baffle Scatter

T.M. Brown
June 8, 2005

ABSTRACT

During the Fall 2004 campaign of thermal-vacuum tests on WFC3, we looked for optical ghosts in the IR channel by imaging a saturated point source at various positions on the detector. For the F110W and F160W filters, 34 positions were checked on and off the detector, while the remaining filters were checked at one position in each quadrant. Although the primary image was 10x oversaturated in these checks, no signs of optical ghosts were seen. In an additional test, we scanned a bright point source across the baffle edges, immediately outside of the IR field of view. These scans showed that strong scattering can occur from the baffle edge, especially along the upper baffle edge. The strongest glints from the baffle edge contained ~20% of the source flux and were spread over a large area of the detector. The baffle installation is under investigation.

Test Setup

The contract end item (CEI) specification for optical ghosts on WFC3 dictates that no discrete ghost should contain more than 0.1% of the source flux. For the ghost tests, we illuminated the WFC3 IR channel with a point source that was approximately ten times oversaturated (i.e., ~1,000,000 e^- in the peak pixel), so that a discrete ghost exceeding the CEI specification could be detected easily (since it would exceed 1000 e^- in its peak pixel if it was point-like). The point source was generated by the CASTLE optical stimulus,

using the tungsten lamp and 10 micron pinhole. This was done at 34 positions, on and off the detector, for the two filters expected to receive the most use: the F110W and F160W.

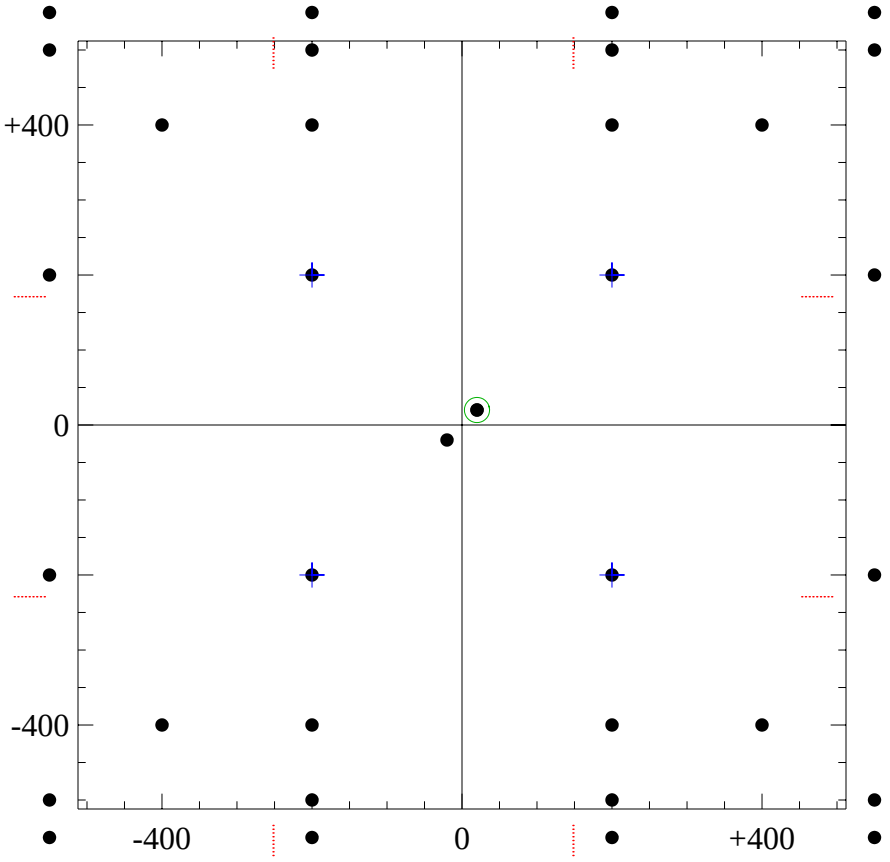

Figure 1: The commanded positions for the ghost and scattered light checks on the IR channel. Black circles mark the locations checked with a saturated source in the F110W and F160W filters; of course, when the source was moved off the detector, the image did not actually saturate. Blue crosses are superimposed on the subset of those locations checked in the remaining filters. A green circle marks the location of the unsaturated image in each filter, used for determining the flux of the source. The red dots mark the edge-to-baffle scans in the F160W filter.

For each of the remaining filters (excluding the grisms), we illuminated one position in each of the four detector quadrants. Besides these standard checks for ghosts, we obtained additional images in the F160W filter to look for scattered light from the baffle encircling the IR detector. These scattered light tests moved the source from the detector edge outward, past the edge of the baffle, at two locations along each detector edge.

The commanded positions are shown in Figure 1. Due to the alignment of the IR channel, the observed positions (Figure 2) are typically offset from the commanded positions

by approximately 50 pixels in X (toward the right) and 30 pixels in Y (toward the top); because the scan from edge to baffle required precise positioning of the source, the alignment offset was taken into account when selecting the commanded positions, so that the observed positions would come out in the desired locations. For each filter, a STEP50 full-frame (1024x1024 pixels) sequence was performed at each of the positions tested in that filter, followed by a RAPID subarray (256x256 pixels) sequence near field center to provide an indication of the count rate using unsaturated readouts.

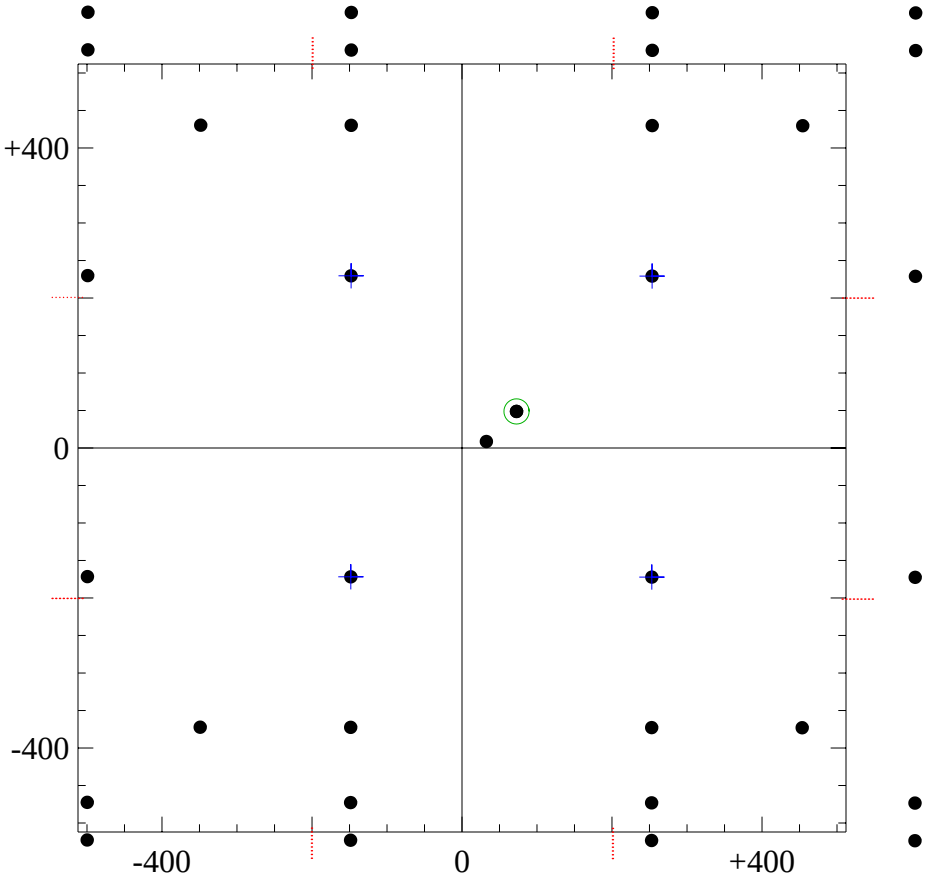

Figure 2: The same as in Figure 1, but now showing the approximate observed locations of the source (instead of the commanded locations). These locations are offset by ~50 pixels in X and ~30 pixels in Y.

Analysis

First we estimated how many counts would have appeared in the saturated images of the source if the images had not saturated. To do this, we took the contemporaneous unsaturated image in each filter and performed aperture photometry (5 pixel radius and 15-20 pixel background annulus) in each of the reads in the RAPID sequence; because some of these sequences began to saturate beyond the fifth read, we performed a linear fit to the

first 5 reads and thus obtained the count rate. The resulting count rate in the source was then scaled by the total exposure time in the saturated images taken in that filter. The results are shown in Table 1. This test aimed for easy detectability of ghosts exceeding the 0.1% level. Given that the primary image of the source exceeded 1,000,000 e^- in all cases, such ghosts would contain at least 1,000 e^-, and thus they would be easily detectable in the data if they were compact.

Table 1. Source signal in the saturated images, had they not saturated.

Filter	e^- (millions)
F093W	8.0
F098M	7.3
F105W	4.7
F110W	6.7
F125W	4.8
F126N	4.7
F127M	4.5
F128N	5.5
F130N	5.9
F132N	5.8
F139M	4.4
F153M	4.0
F160W	6.3
F164N	4.7
F167N	4.8

After obtaining the above estimates of the source strength in the saturated images of each filter, we next visually inspected each of the saturated images by eye to look for optical ghosts. To ease the detectability of any optical ghosts, we subtracted the first read from the last read in each STEP50 sequence (thus removing bias structure), and then subtracted from each image another image from the same filter, but with the source at a distinct position, providing a dark subtraction (thus removing hot and warm pixels). In Figure 3, we show the 200x200 pixel area around the source in each of the four positions sampled for every filter (blue crosses in Figures 1 & 2). Note that the vertical feature immediately above the source is an artifact from the CASTLE optical stimulus, and not an optical ghost due to WFC3.

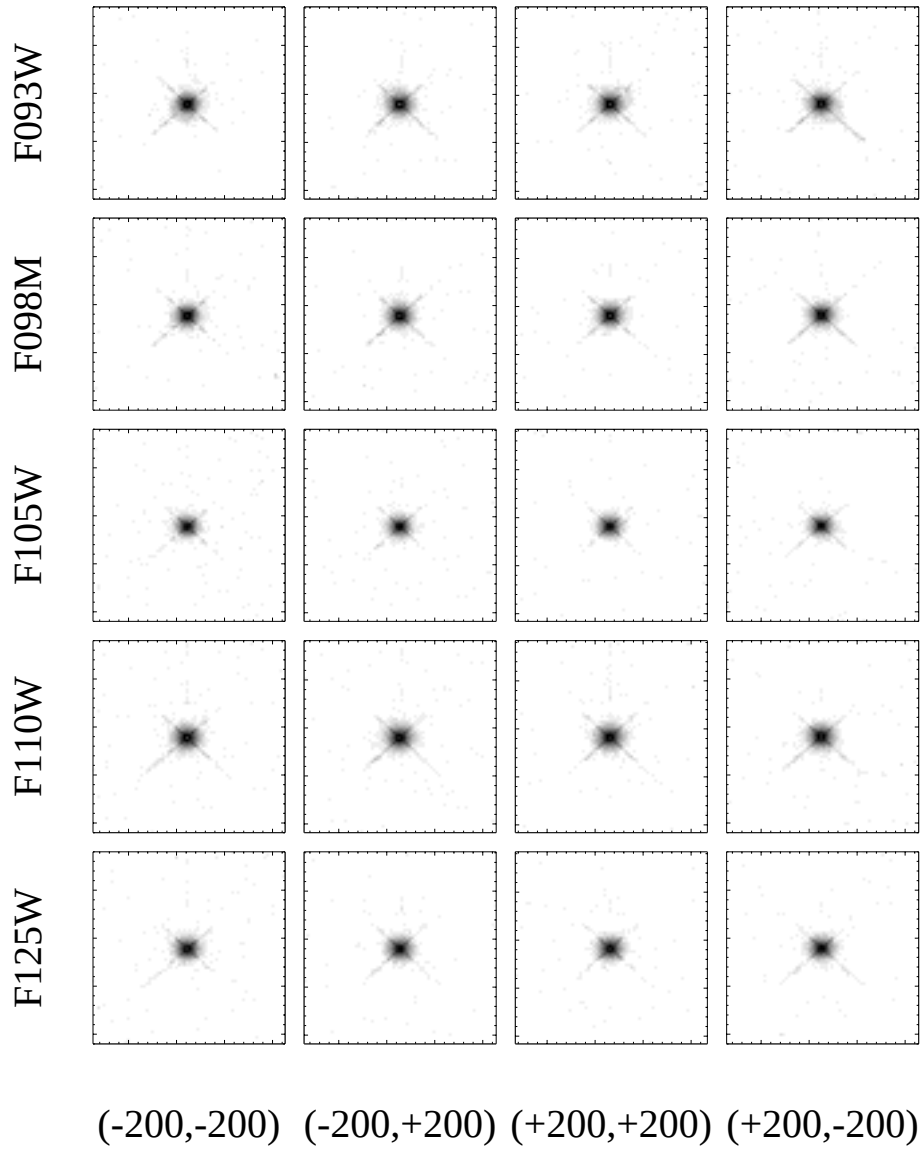

Figure 3: The saturated images taken in the center of each quadrant for each of the WFC3 IR filters, with a hard logarithmic stretch. No optical ghosts can be seen. The vertical feature above the source is an artifact from the CASTLE optical stimulus. The labeled positions are the commanded positions, which are generally offset from the observed positions by ~50 pixels in X and ~30 pixels in Y (see Figures 1 & 2).

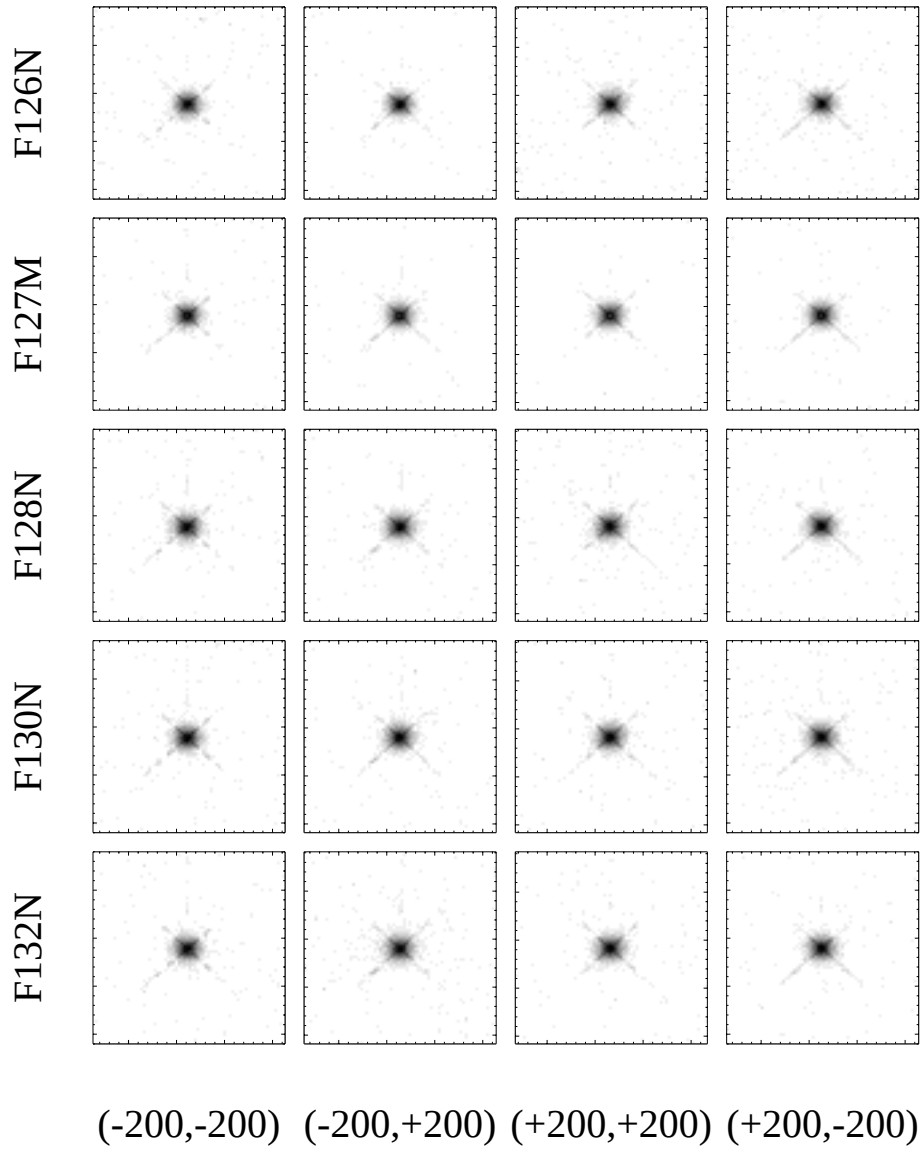

Figure 3: Continued.

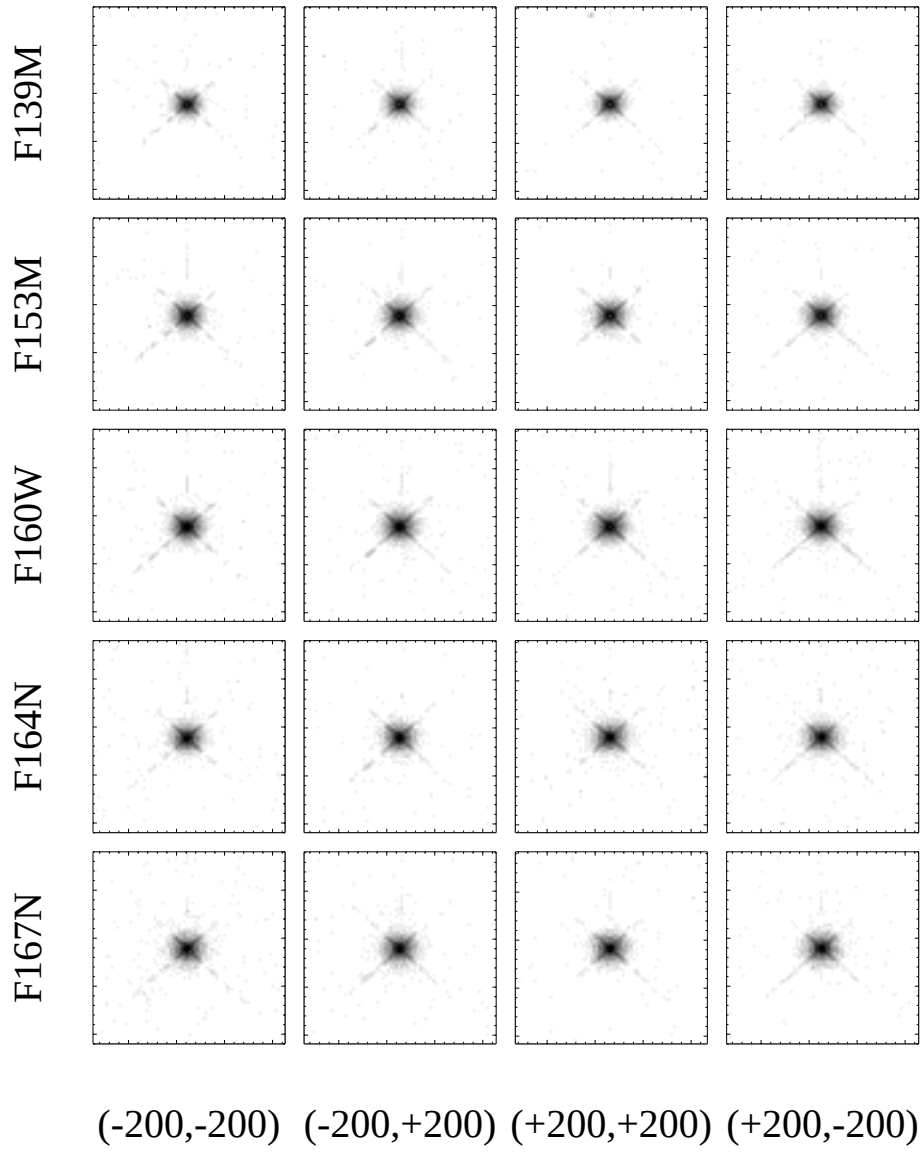

Figure 3: Continued.

None of these images showed serious ghosts, but a few filters showed faint ghosts, and a handful of images with the source placed near the edge of the detector (both on and off the detector) showed signs of scattered light:

- The F093W images showed faint rings superimposed on the wings of the PSF (Figure 3), but it was difficult to measure their strength accurately, given their proximity to the source. We attempted a measurement by taking a region enclosing the rings and comparing the counts therein to those in a region of identical size on the other side of the PSF, but this comparison gave no excess counts in the region containing the ghosts.
- There was also a hint of such rings in the F126N images (Figure 3), but as with the case of the F093W images, the rings were superimposed on the wings of the PSF and difficult to quantify. These rings were even fainter than in the case of the F093W, and somewhat confused with the interference pattern in this narrow-band filter.
- The F110W image of the source commanded to (-200,+400) showed no optical ghosts in the immediate vicinity of the primary image, but did show a possible glint ~110 pixels away (Figure 4), almost along the upper-left diffraction spike. Because the source was on the detector, it is unclear what was causing the glint. It is almost certainly not a ghost, because one would expect a similar feature to show up in some of the other F110W images (which were taken at numerous field points). It might be a cosmic ray or a glint from the diffraction spike hitting the upper baffle edge. By comparing the counts in a 20x20 pixel region centered on this glint to such regions in surrounding areas, we estimated that the glint contained ~0.5% of the source flux.
- The F110W image of the source commanded to (-200,+500) placed the source off the top edge of the detector (due to the alignment offset) and near the baffle edge (located approximately 50 pixels beyond the detector edge). An extended glint containing ~0.6% of the source flux was seen ~120 pixels below the detector edge (Figure 5). Commanding the source to (-550,+500) also caused a very diffuse glint with a stronger linear patch in it containing 0.5% of the source flux (Figure 6). A much stronger and extended glint appeared when the source was commanded to (+200,+500), with ~7% of the source flux appearing in the glint (Figure 7).
- Similar glints were seen in the F160W images, although some were stronger because here we scanned the source across the baffle edge with very small increments, allowing a “peak up” on the location with the strongest scattering. As with the F110W images, significant glints were seen along the baffle edge near top of the detector, such as the ~2% glint with the source commanded to (-200,+500) and the ~5% glint with the source commanded to (+148,+501); see Figures 8 and 9, respectively. Along the same edge, much stronger glints (~20%) were seen when the source was commanded to (+200,+500) and (-252,+501); see Figures 10 & 11, respectively. A small motion to (-252,+506) showed the glint dropping off to ~4% of the source flux (Figure 12). These glints were not restricted to the top edge of the detector; when the source was commanded to (+148,-559), a glint at ~4% of the source flux appeared (Figure 13). Weak glints (~1%) also appeared well-separated from the source by hundreds of pixels, which happened when the source was moved to (+148,+481) and (+468,+171); see Figures 14 & 15.

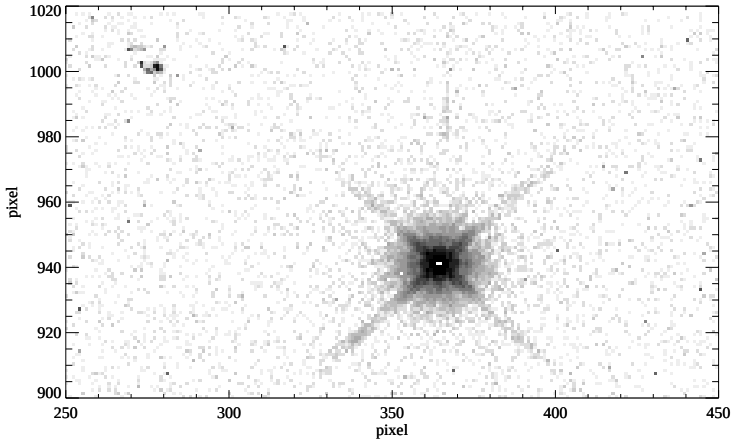

Figure 4: Logarithmic image with the F110W filter. There was an apparent 0.5% glint associated with the point source located on the detector but near the upper edge.

Figure 5: F110W image with same logarithmic stretch as Figure 4. A 0.6% glint appeared when the source was moved near the upper baffle edge, which is located about 50 pixels beyond the detector edge.

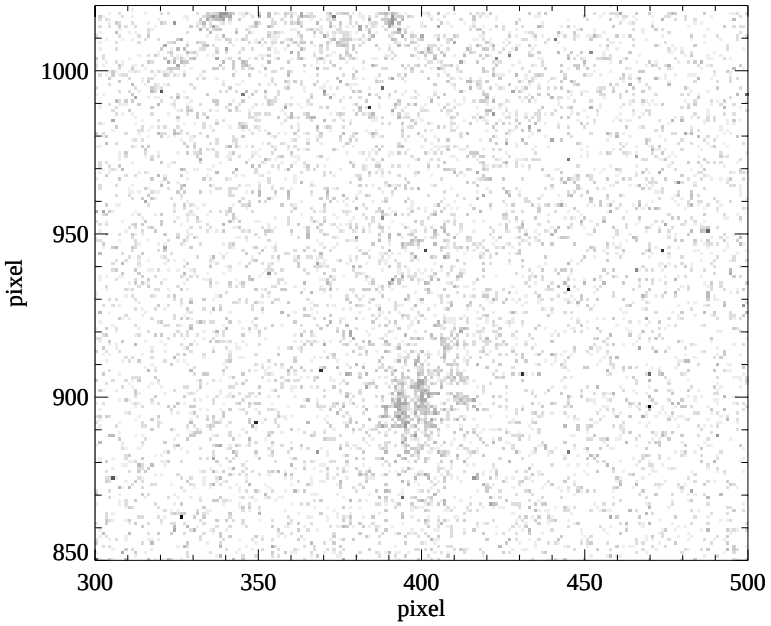

Figure 6: F110W image with same logarithmic stretch used in Figures 4-5. With the source placed near the upper baffle edge but to the upper left of the detector, there was an extremely diffuse glint and a brighter linear patch at 0.5%.

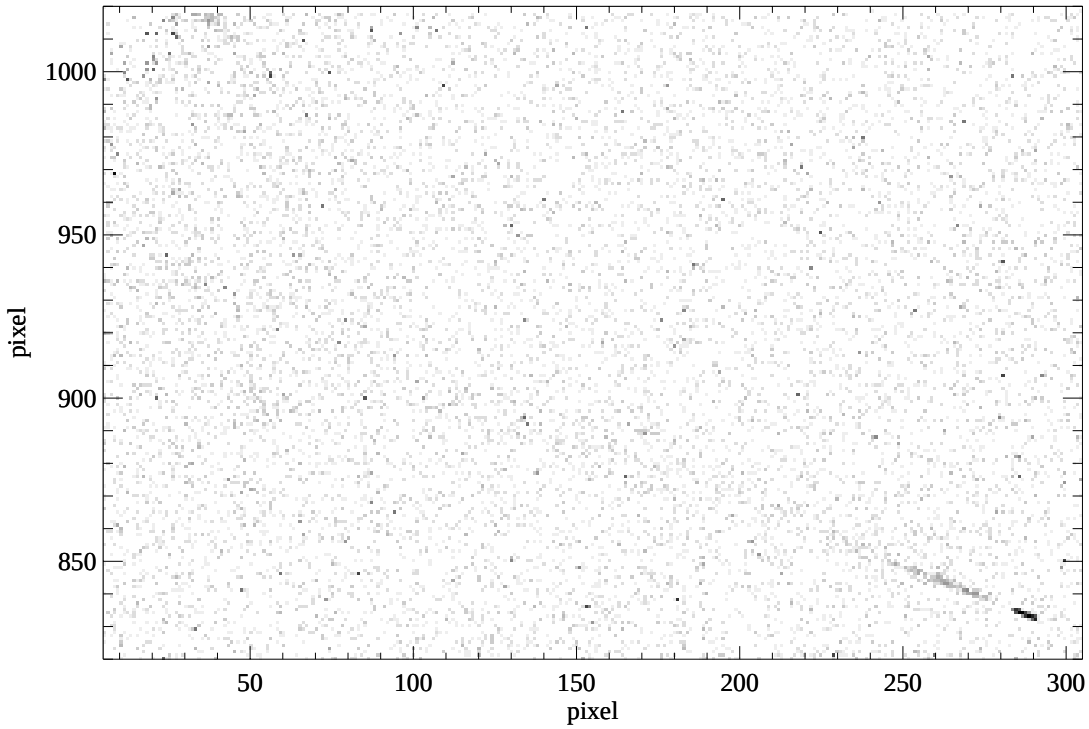

Figure 7: F110W image with the same log stretch used in Figures 4-6, showing a strong (7%) glint caused by a point source on the upper baffle edge.

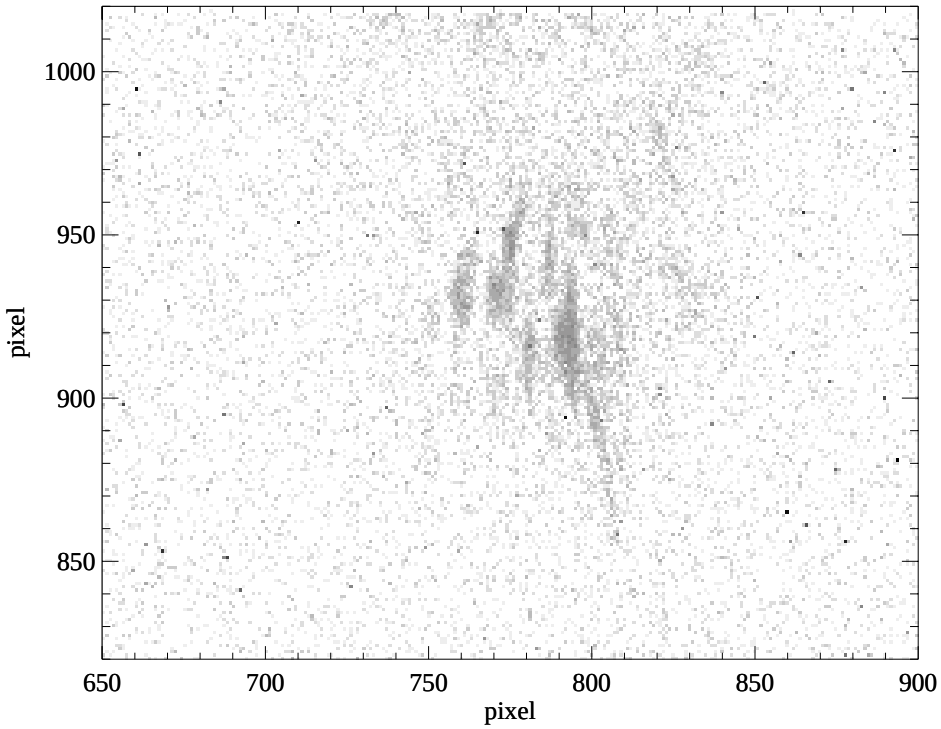

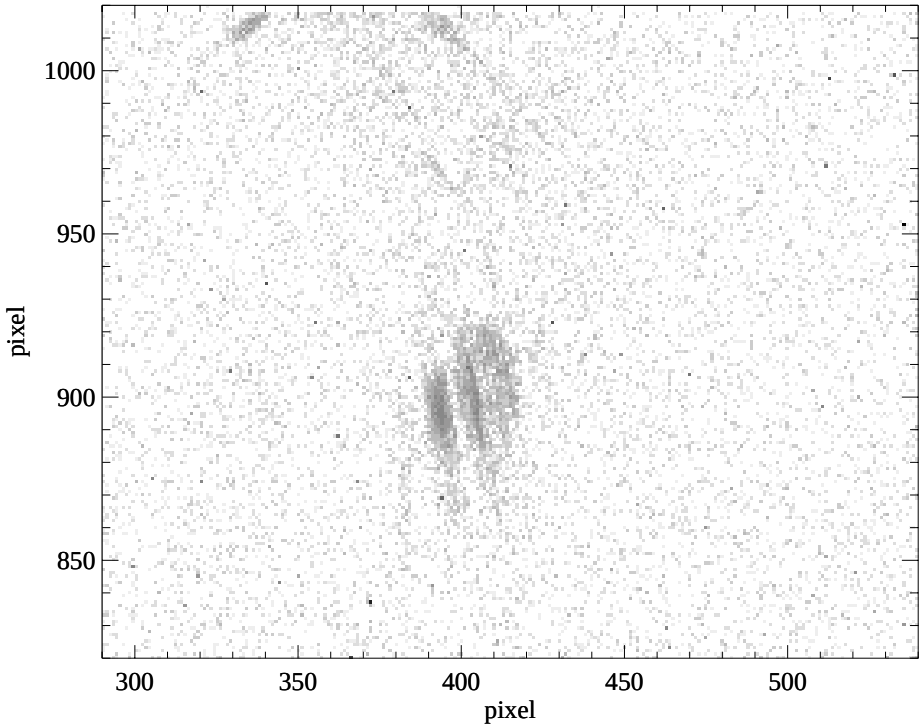

Figure 8: F160W image with the same log stretch used in Figures 4-7, showing a significant glint (2%) caused by a point source on the upper baffle edge.

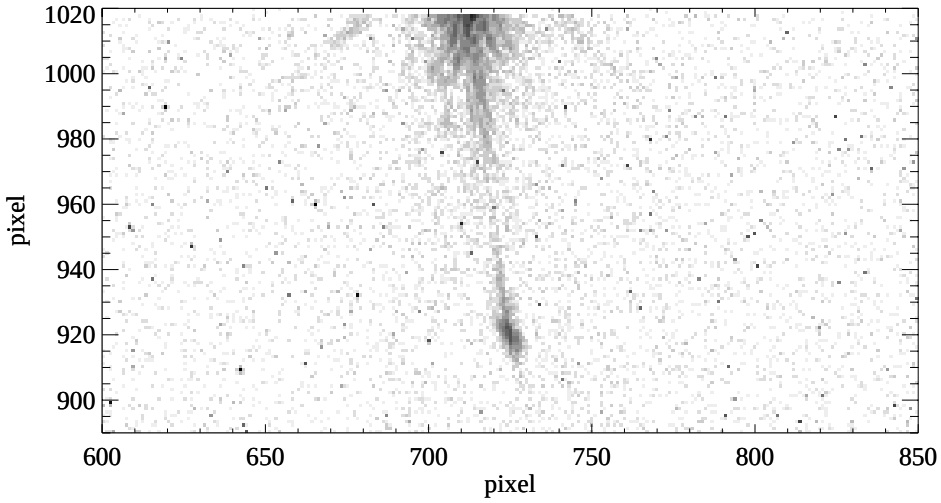

Figure 9: As in Figure 8, but for another position along the upper baffle edge.

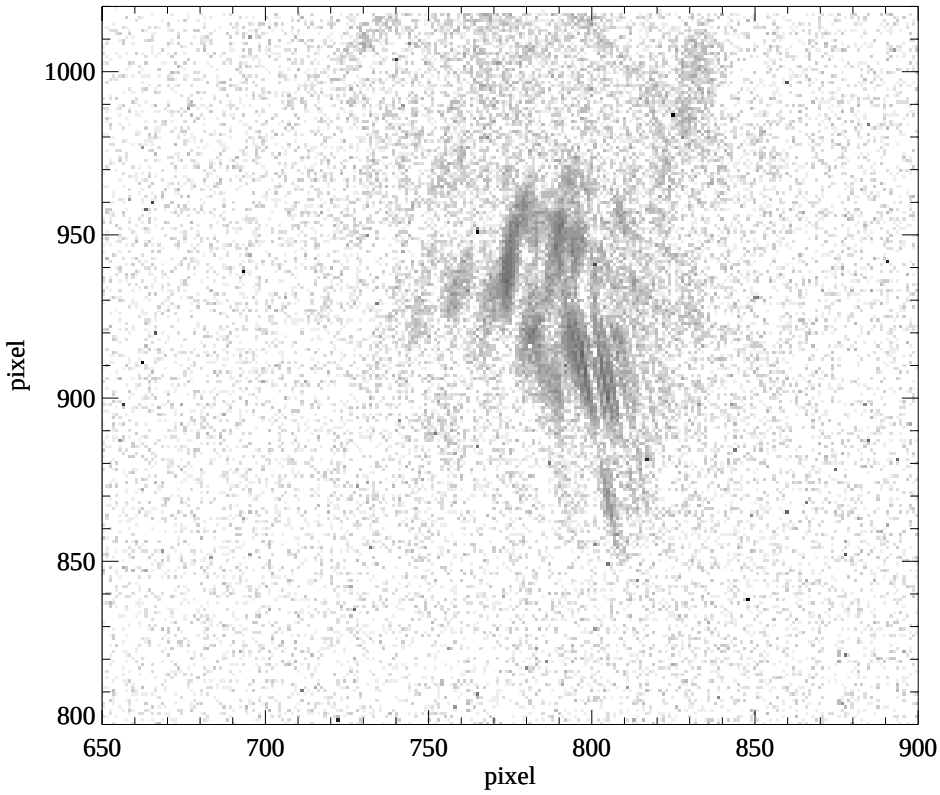

Figure 10: F160W image with the same log stretch used in Figures 4-9, showing an extremely strong glint (nearly 20%) when the source was commanded to (+200,+500). The upper baffle edge consistently showed the strongest scatter.

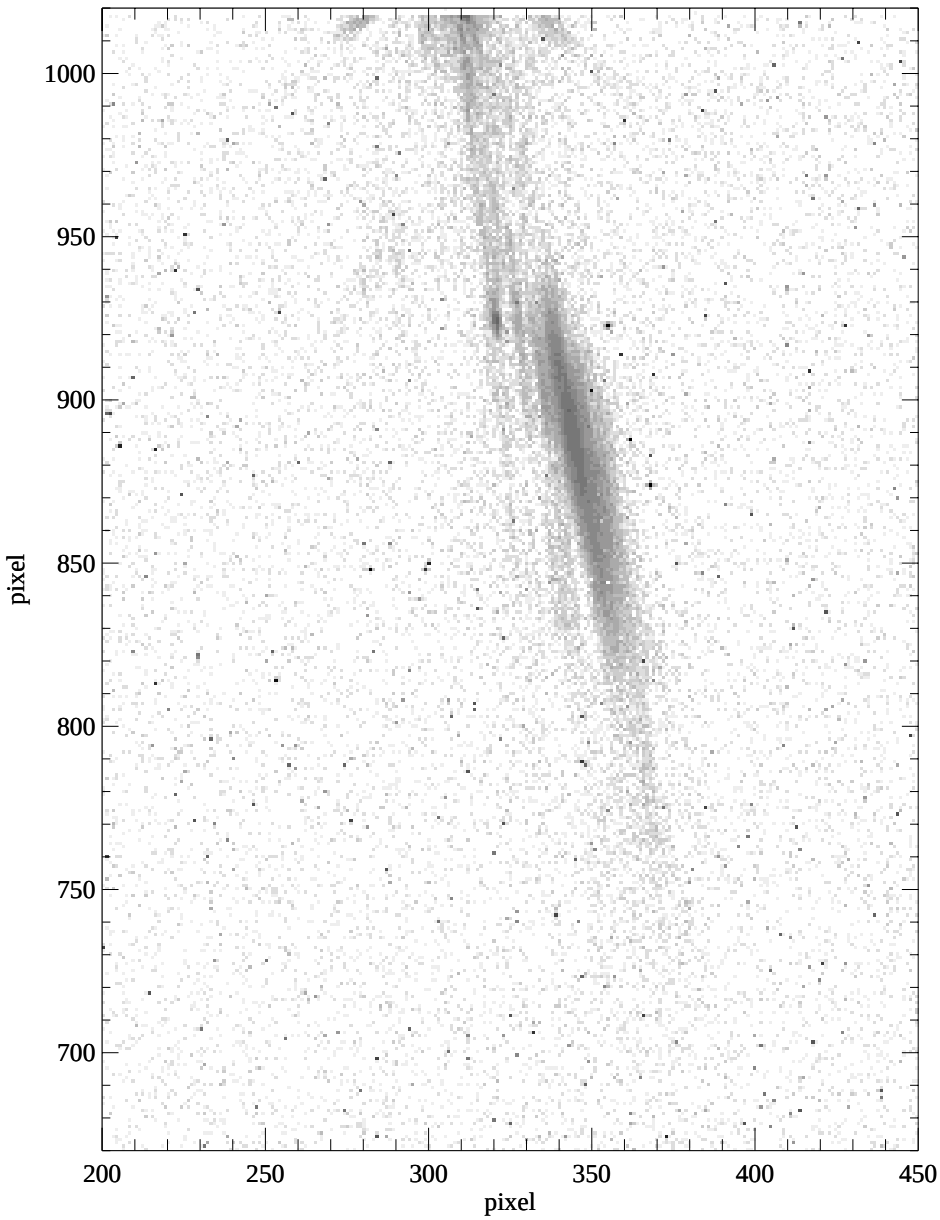

Figure 11: F160W image with the same log stretch used in Figures 4-10, showing another strong (~20%) glint produced by a source on the upper baffle edge. The surface brightness of the glint reaches ~10 e^-/s/pixel, compared to ~10^5 e^-/s in the source (which is roughly the count rate one would expect from a K0V star at V=13 mag).

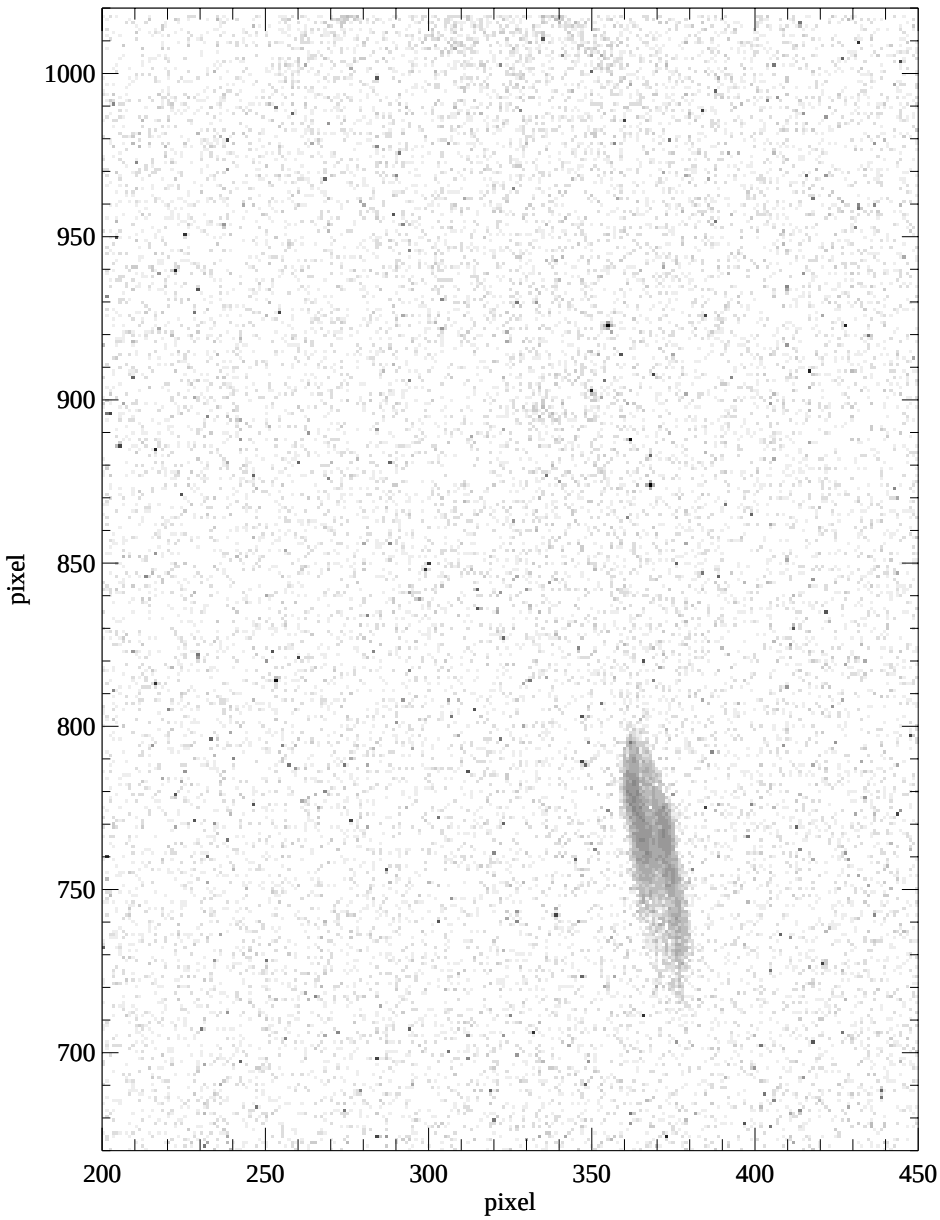

Figure 12: The same section of the detector shown at the same log stretch as used in the previous figure, but the source was moved 5 pixels upward, showing a rapid decline in the scattering; the glint dropped to 4% of the source flux.

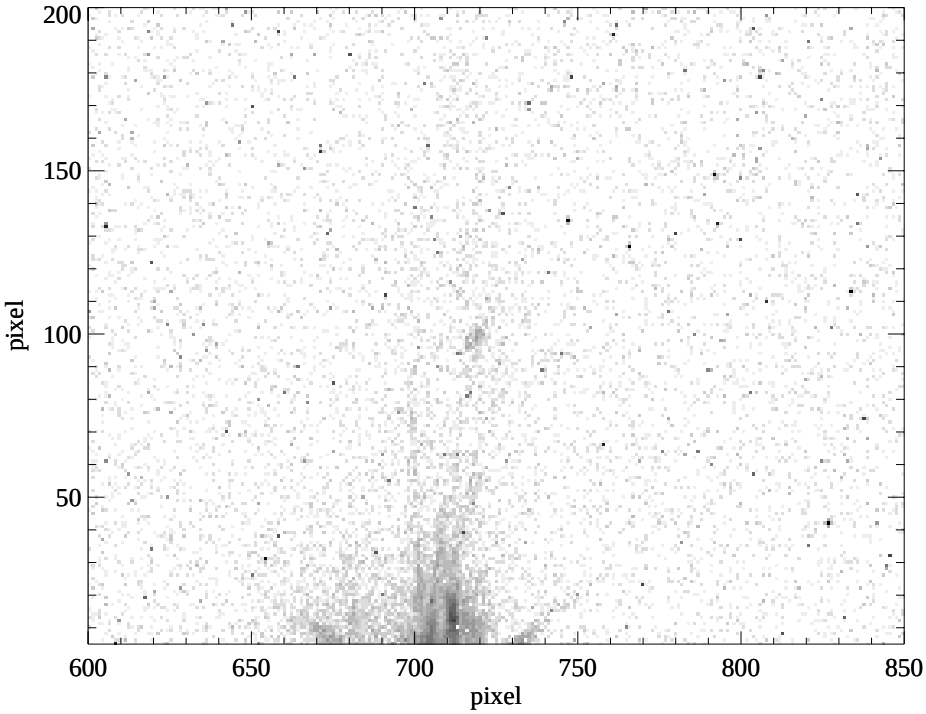

Figure 13: F160W image shown at the same log stretch used in Figures 4-11. The upper baffle edge is not the only source of significant scattering. Here, the source fell on the lower baffle edge, producing a glint at ~4% of the source flux.

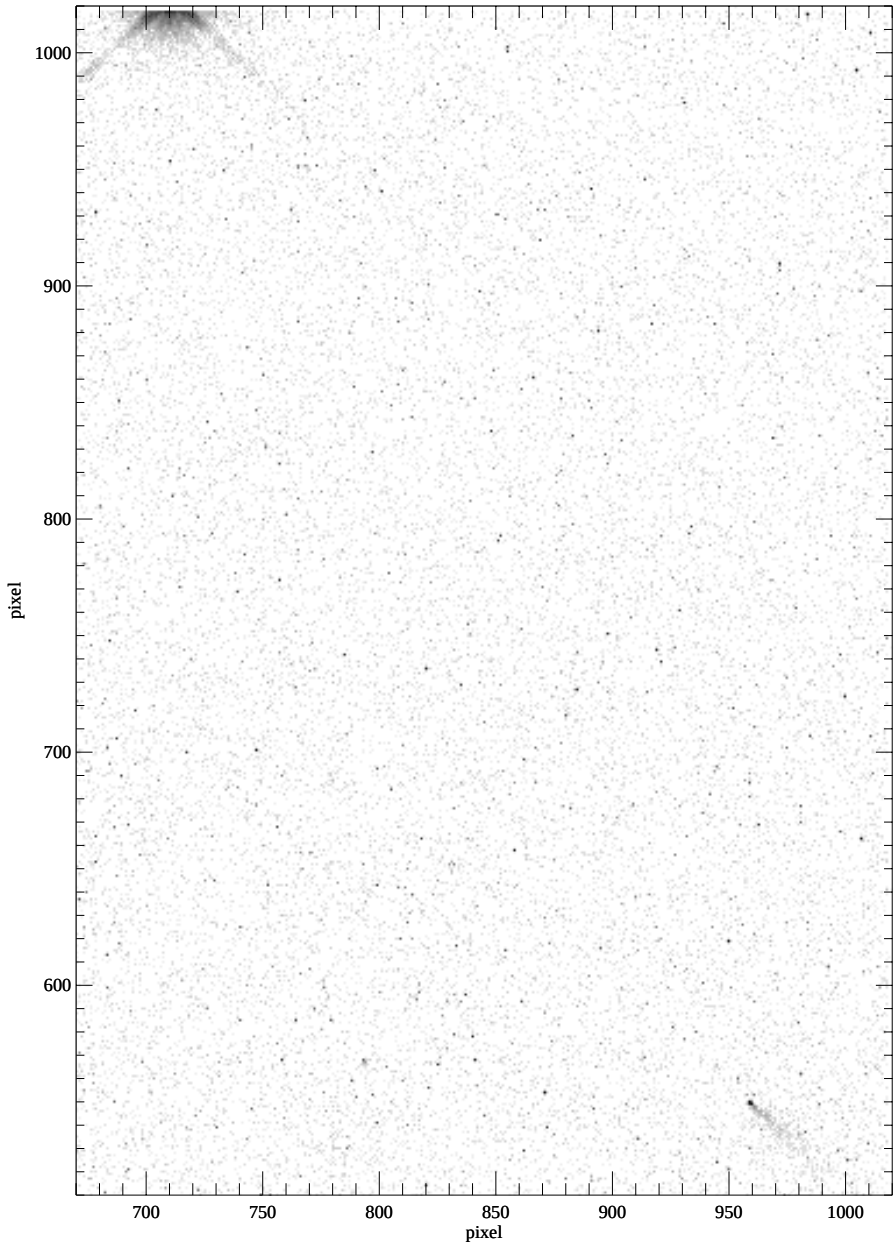

Figure 14: F160W image shown at the same log stretch as Figures 4-13, but reduced in scale. Glints appeared well-separated from the source by hundreds of pixels.

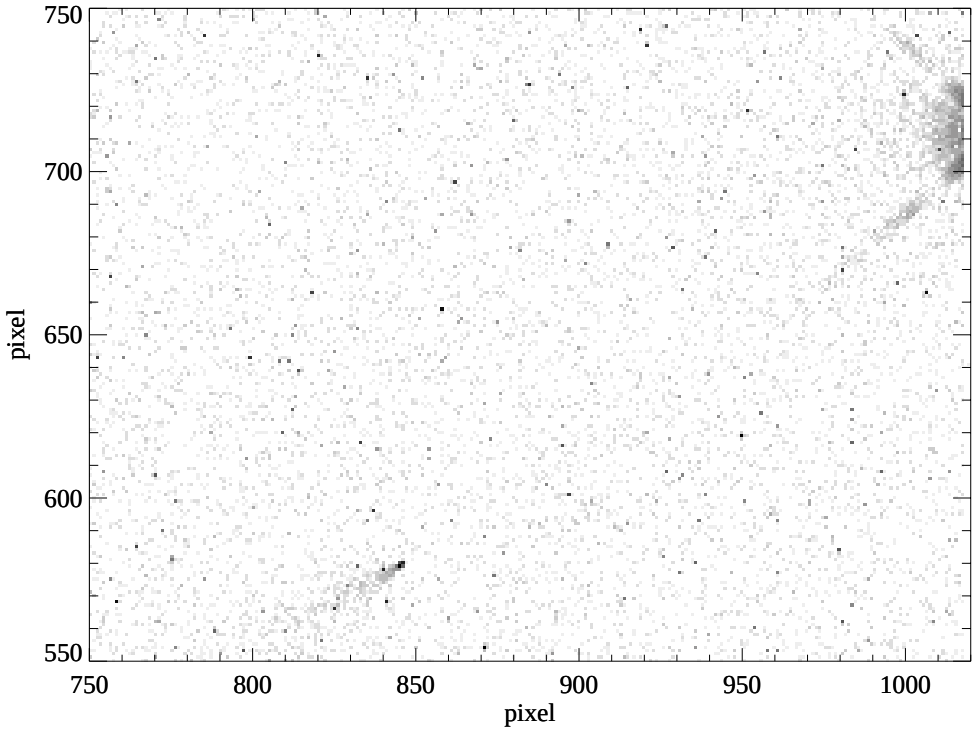

Figure 15: F160W image shown at the same logarithmic stretch used in Figures 4-14, showing another glint well-separated from the source.

Discussion

Although no serious optical ghosts appeared in our tests, it is clear that the detector baffle can cause significant scatter, particularly from the upper baffle edge. The strength of the glint from this baffle varied strongly (from ~1% to ~20%) with very small changes in source position (a few pixels). Although the total flux in the glint was sometimes very large, it was spread over a large image area, and thus the surface brightness was relatively low. However, in-flight imaging of crowded fields may result in multiple sources hitting the baffle edge, causing increased background and a significant degradation in performance. It is now thought that the baffle may have been installed incorrectly in the IR detector package; this is under investigation.